Published in final edited form as:
J Biomech. 2012 April 5; 45(6): 1117–1122. doi:10.1016/j.jbiomech.2011.12.025.

A methodology to accurately quantify patellofemoral cartilage contact kinematics by combining 3D image shape registration and cine-PC MRI velocity data

Bhushan S. Borotikar, D.Eng[1], **William H. Sipprell III, BS**[2], **Emily E. Wible, BS**[1], and **Frances T. Sheehan, PhD**[1]

[1]Functional and Applied Biomechanics, Department of Rehabilitation Medicine, NIH, Bethesda, MD, USA

[2]University at Buffalo, School of Medicine and Biomedical Sciences, Buffalo, NY, USA

Abstract

Patellofemoral osteoarthritis and its potential precursor patellofemoral pain syndrome (PFPS) are common, costly, and debilitating diseases. PFPS has been shown to be associated with altered patellofemoral joint mechanics; however, an actual variation in joint contact stresses has not been established due to challenges in accurately quantifying *in vivo* contact kinematics (area and location). This study developed and validated a method for tracking dynamic, *in vivo* cartilage contact kinematics by combining three magnetic resonance imaging (MRI) techniques, cine-phase contrast (CPC), multi-plane cine (MPC), and 3D high-resolution static imaging. CPC and MPC data were acquired from 12 healthy volunteers while they actively extended/flexed their knee within the MRI scanner. Since no gold standard exists for the quantification of *in vivo* dynamic cartilage contact kinematics, the accuracy of tracking a single point (patellar origin relative to the femur) represented the accuracy of tracking the kinematics of an entire surface. The accuracy was determined by the average absolute error between the PF kinematics derived through registration of MPC images to a static model and those derived through integration of the CPC velocity data. The accuracy ranged from 0.47mm–0.77mm for the patella and femur and 0.68mm–0.86 mm for the patellofemoral joint. For purely quantifying joint kinematics, CPC remains an analytically simpler and more accurate (accuracy < 0.33mm) technique. However, for application requiring the tracking of an entire surface, such as quantifying cartilage contact kinematics, this combined imaging approach produces accurate results with minimal operator intervention.

Keywords

knee; MRI; dynamic; femur; patella; contact kinematics

Corresponding author: Frances T. Sheehan, PhD, National Institutes of Health, Building 10 CRC RM 1-1469, 10 Center Drive MSC 1604, Bethesda, MD 20892-1604, Tel: (301) 451-7585, fsheehan@cc.nih.gov.

Conflict of interest statement
No authors have any conflict of interest to report.

INTRODUCTION

Patellofemoral osteoarthritis, although less studied than tibiofemoral osteoarthritis, is a common pathology (Thorstensson et al., 2009), particularly in elderly women and has been correlated directly with disability (McAlindon et al., 1992). Patellofemoral pain syndrome (PFPS), a potential precursor of patellofemoral osteoarthritis (Utting et al., 2005), can be just as disabling in the adolescent and young adult years (Boling et al., 2009). It is hypothesized that alterations in patellofemoral joint mechanics (Andriacchi and Mundermann, 2006; Hunter et al., 2007; Sheehan et al., 2009; Wilson et al., 2009) lead to pain and ultimately to joint degeneration. Thus, being able to accurately quantify cartilage contact mechanics is critical for advancing the prevention and treatment of both pathologies. Unfortunately, direct quantification of dynamic joint contact parameters in patients with these pathologies has yet to be demonstrated.

Due to the challenges associated with quantifying *in vivo* patellofemoral contact mechanics, most knowledge regarding joint contact mechanics have been garnered from cadaveric data (Elias et al., 2011; Gorniak, 2009; Guterl et al., 2009) and more recently, from computational modeling (Cohen et al., 2003; Farrokhi et al., 2011; Lin et al., 2010). The clinical utility of cadaveric studies is severely limited by uncertainty in emulating accurate *in vivo* physiological loading conditions and pathological alterations. Similar uncertainties and a lack of validation limit computational modeling. Previous studies (Connolly et al., 2009; Ward et al., 2007) have estimated patellofemoral contact areas and locations using static magnetic resonance imaging (MRI). Such *in vivo* measures will likely help advance the clinical understanding of PFPS and patellofemoral osteoarthritis, but fall short due to their inability to incorporate dynamic conditions.

Thus, the overall goal of this project is to develop an MRI-based experimental and analytical toolset that can accurately and non-invasively track *in vivo*, dynamic patellofemoral joint contact mechanics. As part of this overall goal, the current study developed a methodology for tracking dynamic *in vivo* cartilage contact kinematics, defined as temporally dependent cartilage contact areas and locations (Yao et al., 2008). This was accomplished by combining three MR imaging techniques, cine-phase contrast (CPC), multi-plane cine (MPC), and 3D high-resolution static imaging. CPC MRI is a dynamic imaging technique that captures a series of anatomic images, along with the corresponding 3D velocity of each voxel within the image, across a motion cycle (Sheehan et al., 1998). Despite its sub-millimeter accuracy (<0.33mm/0.97°) and excellent precision (<0.18°) (Behnam et al., 2011) in tracking musculoskeletal kinematics (CPC-kinematics), CPC is limited in its ability to provide 3D spatial data. On the other hand, MPC generates temporally dependent, sparse 3D spatial data, acquired over a movement cycle (Appendix A). Registering the 3D dynamic MPC data to the high resolution 3D static MRI data should enable accurate quantification of cartilage contact kinematics, which is a necessary first step in quantifying contact mechanics. Since no gold standard exists for the quantification of *in vivo* dynamic cartilage contact kinematics, the accuracy of tracking a single point (patellar origin relative to the femur) was assessed in the current study, as a surrogate for quantifying the accuracy of tracking the kinematics of an entire surface.

METHODS

Twelve healthy volunteers (8F/4M, age = 24.3±5.8years, height = 170.1±9.7cm, weight = 65.1±14.1kg) provided informed consent prior to participating in this IRB approved study. All subjects had no previous lower leg surgery, pathology, long-term pain, and no contra-indications to having an MR scan.

Subjects lay supine within a 3T MRI scanner (Philips Medical Systems, Best, NL) as a series of dynamic and static scans were acquired. For the dynamic scans, the subjects' knees were placed on a cushioned block within an MRI-compatible fixture with flexible transmit-receive coils securely placed around the knee. While the subjects extended and flexed their knees (30 cycles per minute) to the beat of a metronome, three dynamic scans (sets of 24 time-frames each) were acquired: **1)** a sagittal-oblique CPC image set (x, y, and z velocity data and anatomical image data), **2)** a sagittal-oblique MPC image set (5–7 anatomical planes per time frame without corresponding velocity data), and **3)** an axial MPC image set (Table 1). The latter was used for establishing anatomical coordinate systems (Seisler and Sheehan, 2007). Subsequently, the subjects' knees were fully extended and placed in an 8-channel knee coil to collect high resolution static 3D sagittal Gradient Recall Echo (GRE) images (Table 2).

The CPC-kinematics were derived as previously reported (Seisler and Sheehan, 2007). For the MPC-kinematics, static 3D models were generated from the high-resolution 3D GRE images with and without fat-suppression for the femur and patella, respectively. The image types selected optimized the contrast between the cortical bone and the surrounding tissue. Three-dimensional static point clouds were created by manually segmenting the outer cortical bone contours using MIPAV (Medical Image Processing and Visualization, NIH, Bethesda, MD). These point clouds were then imported into Geomagic 3D modeling software (Geomagic Inc., Research Triangle Park, NC), fitted with a triangular polynomial surface, and smoothed (maximum smoothing = 0.2mm). Similarly, sparse dynamic femoral and patellar models were created by manually segmenting the respective bones from the MPC image data for each time frame. The 24 point clouds for each bone were then imported into Geomagic and fitted to their respective 3D static model using an iterative closest point algorithm. The transformation matrices defining the 3D spatial relationship between the static model and dynamic point cloud were saved for each bone at each of the 24 time frames (Figure 1). Through matrix multiplication, the MPC-kinematics were quantified over time. Both the MPC- and CPC-kinematics were expressed in terms of the identical anatomical coordinate system (Figure 2). Since integration was an inherent low-pass filter, the MPC-kinematics were filtered using a low-pass butterworth filter (2^{nd} order with cutoff frequency of 0.25Hz.) in MATLAB (Mathworks Inc. Natick, MA).

Registration between the high-resolution 3D static MR data and a single time-frame of data from the MPC dataset was sufficient to define the pose of the static bones and cartilage within the dynamic space (Figure 3). Once this was done, CPC-kinematics could be used to define the change in orientation and position of these bodies throughout the movement. However, registration could also be performed using all 24 time frames of the MPC data, enabling the MPC-kinematics to be derived over the entire movement cycle without the use of the CPC data. This redundancy of data was used to evaluate the accuracy of quantifying the kinematics of points of interest on the patella and femur and allowed two methodological approaches to be investigated. The first relied solely on the MPC registration to quantify cartilage contact kinematics and the second relied on registering a single time frame of the MPC data combined with the CPC data to quantify cartilage contact kinematics.

Accuracy was defined as the average absolute error between the CPC- and MPC-kinematics (Figure 1). Two such accuracies were defined: 1) $\mathbf{accuracy_{All}}$, which represented the accuracy of the MPC registration technique in isolation to track 3D patellofemoral translation. This calculation incorporated all 24 times frames, and 2) $\mathbf{accuracy_{QS}}$, which represented the accuracy of using MPC registration from a single time frame in combination with the CPC-kinematics to track 3D patellofemoral translation. Instead of simply reporting the time frame with the lowest error, $\mathbf{accuracy_{QS}}$ incorporated all the quasi-static (QS) time-frames, where the knee angle changed less than 1.75°/time-frame. These time frames contain

the least temporal averaging, and would be the most logical choice for use in a single-time frame registration process. For completeness, the accuracy of tracking the 3D orientation of the patellofemoral joint was also reported.

RESULTS

Qualitatively analysis of the contact patterns of the healthy volunteers produced reasonable results (Figure 3), demonstrating the feasibility applying the registration methodology to determine cartilage contact kinematics.

There was a good agreement between the CPC- and MPC-kinematics (Figure 4). The **accuracy$_{QS}$** ranged from 0.47mm–0.77mm for the patella and femur. For the patellofemoral joint, the **accuracy$_{QS}$** ranged from 0.68mm–0.86mm (Table 3). The errors associated with the combined MPC and CPC analysis (**accuracy$_{QS}$**) were consistently lower than those associated with the MPC registration alone **(accuracy$_{All}$**).

DISCUSSION

This study presents the only technique that can be used to computationally track *in vivo*, cartilage contact kinematics during a dynamic volitional movement with sub-millimeter accuracy. Based on Li and colleagues' (2011) cadaveric study, this sub-millimeter accuracy would result in 1% or smaller errors in the calculation of total cartilage wear area. The patellofemoral **accuracy$_{QS}$** is comparable to that reported by Fellows and colleagues (2005) for quantifying static patellofemoral alignment by registering a sparse static patellar model to a high quality 3D model.

Since cartilage surface descriptions are readily available from the MR data, the technique reported by Fellows and colleagues could be used to quantify cartilage contact areas and locations with sub-millimeter accuracies for static poses. Bi-plane radiography holds ready potential for quantifying joint contact kinematics with a reported accuracy of ≤ 0.39mm and 0.87° (Bey et al., 2008) for tracking patellofemoral kinematics by matching 2D dynamic flouroscopic projections to a 3D computed tomography (CT) model. However, cartilage is not visible in CT images, limiting the ability of bi-plane radiography to evaluate cartilage contact kinematics. It is further limited by its required ionizing radiation exposure. Replacing the CT with an MRI-based model, enables the visualization of cartilage, but may introduce unacceptably high registration errors. For example, Li and colleagues (2011) recently reported that replacing a laser generated model with an MR image-based model increased the total predicted contact wear area in a cadaveric knee by 13%.

Peak cartilage thickness in healthy adults has been reported to range from 4.5mm–5.5mm in patella and 3.5mm–4mm in femur (Draper et al., 2006; Eckstein et al., 2001), indicating that sub-millimeter accuracies are necessary in order to keep the errors in estimating patellofemoral contact kinematics within acceptable limits. There remains a gap in understanding how the accuracy and precision of contact kinematic measurements affects the estimation of contact mechanics and further research focused on bridging this gap is warranted.

Although the MPC and CPC data were derived from the same modality (MRI), which is common in validation studies (Bey et al., 2008; Fellows et al., 2005), this did not limit the current study. The MPC and CPC techniques use different components of the MRI signal to produce their final data (making them stand alone techniques). Using the same modality enabled the evaluation of dynamic, *in vivo* patellofemoral kinematics with physiological loading over a relatively large set of living subjects. Unlike the CPC methodology, MPC-registration is highly dependent on the shape and size of the bone being tracked, thus the

current accuracy results are not readily applicable to other joints. As with any validation, the errors associated with the comparator (in this case CPC) are potentially embedded within the calculated accuracy. Even assuming the worst case scenario (that the CPC errors are additive), the accuracy would still remain close to 1mm. Another potential limitation was that the study was done using a loaded, but non-weight-bearing, leg extension exercise. Since numerous studies have noted that evaluating the loaded knee joint at or near full extension in a non-weight bearing exercise may be critical for evaluating PFPS (Connolly et al., 2009; Harbaugh et al., 2010; Powers et al., 2003), this is likely not a limiting factor within the current study.

In conclusion, for the isolated quantification of joint kinematics, CPC remains an analytically simpler and more accurate technique (0.33 mm), as compared to the MPC-registration. However, for applications requiring the tracking of an entire surface, as is the case in quantifying cartilage contact kinematics, the most accurate approach is to register a single QS time-frame combined with the CPC-kinematics. Such data would readily serve as kinematic input to 3D dynamic joint contact models. This combined MRI methodology has an advantage over previous registration-based techniques in that the lengthy process of creating and registering the dynamic condition only needs to be performed at a single, instead of all, time frames. The quantification of *in vivo* cartilage contact kinematics during dynamic, loaded, volitional tasks will advance the understanding of cartilage contact mechanics in both healthy and diseased states.

Acknowledgments

This research was supported in its entirety by the Intramural Research Program of the NIH at the Clinical Center at the NIH. The authors wish to thank Sara Sadeghi, Bonnie Damaska, and the Diagnostic Radiology Department at the National Institutes of Health for their support and research time.

References

Andriacchi TP, Mundermann A. The role of ambulatory mechanics in the initiation and progression of knee osteoarthritis. Curr Opin Rheumatol. 2006; 18(5):514–518. [PubMed: 16896293]

Behnam AJ, Herzka DA, Sheehan FT. Assessing the accuracy and precision of musculoskeletal motion tracking using cine-PC MRI on a 3.0T platform. J Biomech. 2011; 44(1):193–197. [PubMed: 20863502]

Bey MJ, Kline SK, Tashman S, Zauel R. Accuracy of biplane x-ray imaging combined with model-based tracking for measuring in-vivo patellofemoral joint motion. J Orthop Surg Res. 2008; 3:38. [PubMed: 18771582]

Boling M, Padua D, Marshall S, Guskiewicz K, Pyne S, Beutler A. Gender differences in the incidence and prevalence of patellofemoral pain syndrome. Scand J Med Sci Sports. 2009; 20(8):725–730. [PubMed: 19765240]

Cohen ZA, Henry JH, McCarthy DM, Mow VC, Ateshian GA. Computer simulations of patellofemoral joint surgery Patient-specific models for tuberosity transfer. Am J Sports Med. 2003; 31(1):87–98. [PubMed: 12531764]

Connolly KD, Ronsky JL, Westover LM, Kupper JC, Frayne R. Differences in patellofemoral contact mechanics associated with patellofemoral pain syndrome. J Biomech. 2009; 42(16):2802–2807. [PubMed: 19889417]

Draper CE, Besier TF, Gold GE, Fredericson M, Fiene A, Beaupre GS, Delp SL. Is cartilage thickness different in young subjects with and without patellofemoral pain? Osteoarthritis Cartilage. 2006; 14(9):931–937. [PubMed: 16647278]

Eckstein F, Reiser M, Englmeier KH, Putz R. In vivo morphometry and functional analysis of human articular cartilage with quantitative magnetic resonance imaging--from image to data, from data to theory. Anat Embryol (Berl). 2001; 203(3):147–173. [PubMed: 11303902]

Elias JJ, Kirkpatrick MS, Saranathan A, Mani S, Smith LG, Tanaka MJ. Hamstrings loading contributes to lateral patellofemoral malalignment and elevated cartilage pressures: An in vitro study. Clin Biomech (Bristol, Avon). 2011

Farrokhi S, Keyak JH, Powers CM. Individuals with patellofemoral pain exhibit greater patellofemoral joint stress: a finite element analysis study. Osteoarthritis Cartilage. 2011; 19(3):287–294. [PubMed: 21172445]

Fellows RA, Hill NA, Gill HS, MacIntyre NJ, Harrison MM, Ellis RE, Wilson DR. Magnetic resonance imaging for in vivo assessment of three-dimensional patellar tracking. J Biomech. 2005; 38(8):1643–1652. [PubMed: 15958222]

Gorniak GC. Patterns of patellofemoral articular cartilage wear in cadavers. J Orthop Sports Phys Ther. 2009; 39(9):675–683. [PubMed: 19721211]

Guterl CC, Gardner TR, Rajan V, Ahmad CS, Hung CT, Ateshian GA. Two-dimensional strain fields on the cross-section of the human patellofemoral joint under physiological loading. J Biomech. 2009; 42(9):1275–1281. [PubMed: 19433326]

Harbaugh CM, Wilson NA, Sheehan FT. Correlating femoral shape with patellar kinematics in patients with patellofemoral pain. J Orthop Res. 2010; 28(7):865–872. [PubMed: 20108348]

Hunter DJ, Zhang YQ, Niu JB, Felson DT, Kwoh K, Newman A, Kritchevsky S, Harris T, Carbone L, Nevitt M. Patella malalignment, pain and patellofemoral progression: the Health ABC Study. Osteoarthritis Cartilage. 2007; 15(10):1120–1127. [PubMed: 17502158]

Li L, Patil S, Steklov N, Bae W, Temple-Wong M, D'Lima DD, Sah RL, Fregly BJ. Computational wear simulation of patellofemoral articular cartilage during in vitro testing. J Biomech. 2011; 44(8):1507–1513. [PubMed: 21453922]

Lin YC, Haftka RT, Queipo NV, Fregly BJ. Surrogate articular contact models for computationally efficient multibody dynamic simulations. Med Eng Phys. 2010; 32(6):584–594. [PubMed: 20236853]

McAlindon TE, Snow S, Cooper C, Dieppe PA. Radiographic patterns of osteoarthritis of the knee joint in the community: the importance of the patellofemoral joint. Ann Rheum Dis. 1992; 51(7): 844–849. [PubMed: 1632657]

Powers CM, Ward SR, Fredericson M, Guillet M, Shellock FG. Patellofemoral kinematics during weight-bearing and non-weight-bearing knee extension in persons with lateral subluxation of the patella: a preliminary study. J Orthop Sports Phys Ther. 2003; 33(11):677–685. [PubMed: 14669963]

Seisler AR, Sheehan FT. Normative three-dimensional patellofemoral and tibiofemoral kinematics: a dynamic, in vivo study. IEEE Trans Biomed Eng. 2007; 54(7):1333–1341. [PubMed: 17605365]

Sheehan FT, Derasari A, Brindle TJ, Alter KE. Understanding patellofemoral pain with maltracking in the presence of joint laxity: complete 3D in vivo patellofemoral and tibiofemoral kinematics. J Orthop Res. 2009; 27(5):561–570. [PubMed: 19009601]

Sheehan FT, Mitiguy P. In regards to the ISB recommendations for standardization in the reporting of kinematic data. J Biomech. 1999; 32(10):1135–1136. [PubMed: 10476854]

Sheehan FT, Zajac FE, Drace JE. Using cine phase contrast magnetic resonance imaging to non-invasively study in vivo knee dynamics. J Biomech. 1998; 31(1):21–26. [PubMed: 9596534]

Thorstensson CA, Andersson ML, Jonsson H, Saxne T, Petersson IF. Natural course of knee osteoarthritis in middle-aged subjects with knee pain: 12-year follow-up using clinical and radiographic criteria. Ann Rheum Dis. 2009; 68(12):1890–1893. [PubMed: 19054828]

Utting MR, Davies G, Newman JH. Is anterior knee pain a predisposing factor to patellofemoral osteoarthritis? Knee. 2005; 12(5):362–365. [PubMed: 16146626]

Ward SR, Terk MR, Powers CM. Patella alta: association with patellofemoral alignment and changes in contact area during weight-bearing. J Bone Joint Surg Am. 2007; 89(8):1749–1755. [PubMed: 17671014]

Wilson NA, Press JM, Koh JL, Hendrix RW, Zhang LQ. In vivo noninvasive evaluation of abnormal patellar tracking during squatting in patients with patellofemoral pain. J Bone Joint Surg Am. 2009; 91(3):558–566. [PubMed: 19255215]

Yao J, Lancianese SL, Hovinga KR, Lee J, Lerner AL. Magnetic resonance image analysis of meniscal translation and tibio-menisco-femoral contact in deep knee flexion. J Orthop Res. 2008; 26(5): 673–684. [PubMed: 18183628]

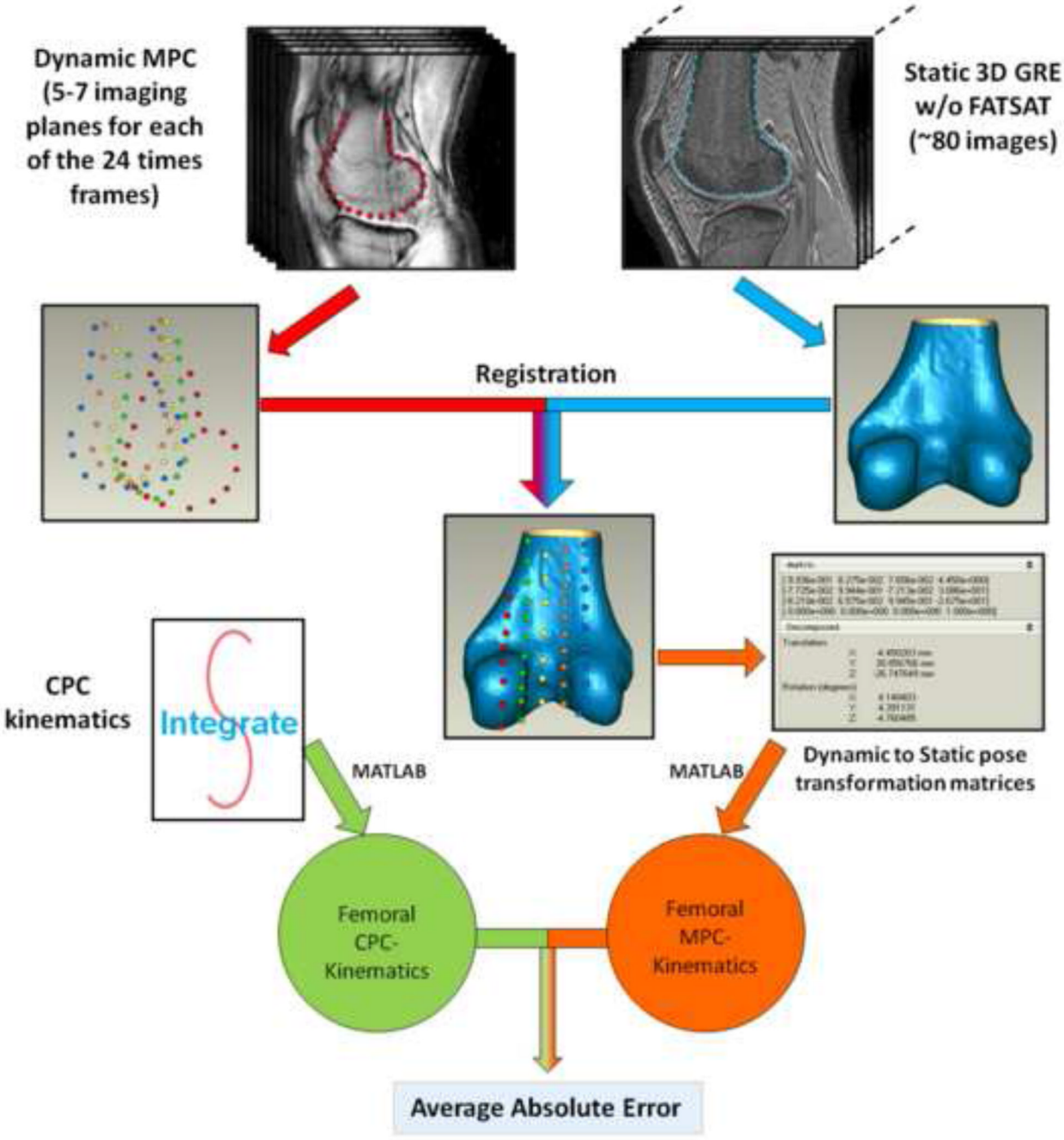

Figure 1. Accuracy analysis

Three-dimensional static point clouds were created by manually segmenting the outer cortical bone contours on both the MPC and the 3D GRE images. These point clouds were then imported into Geomagic. The contours from the 3D GRE image were transformed to a triangular polynomial surface. Each of the 24 point clouds for each bone was then fitted to their respective 3D static model using an iterative closest point algorithm ("Registration"). The transformation matrices defining the 3D spatial relationship between the static model and dynamic point cloud were saved for each bone at each of the 24 time frames. The CPC- and MPC-kinematics were then transformed into the same anatomical coordinate system before calculating the absolute error.

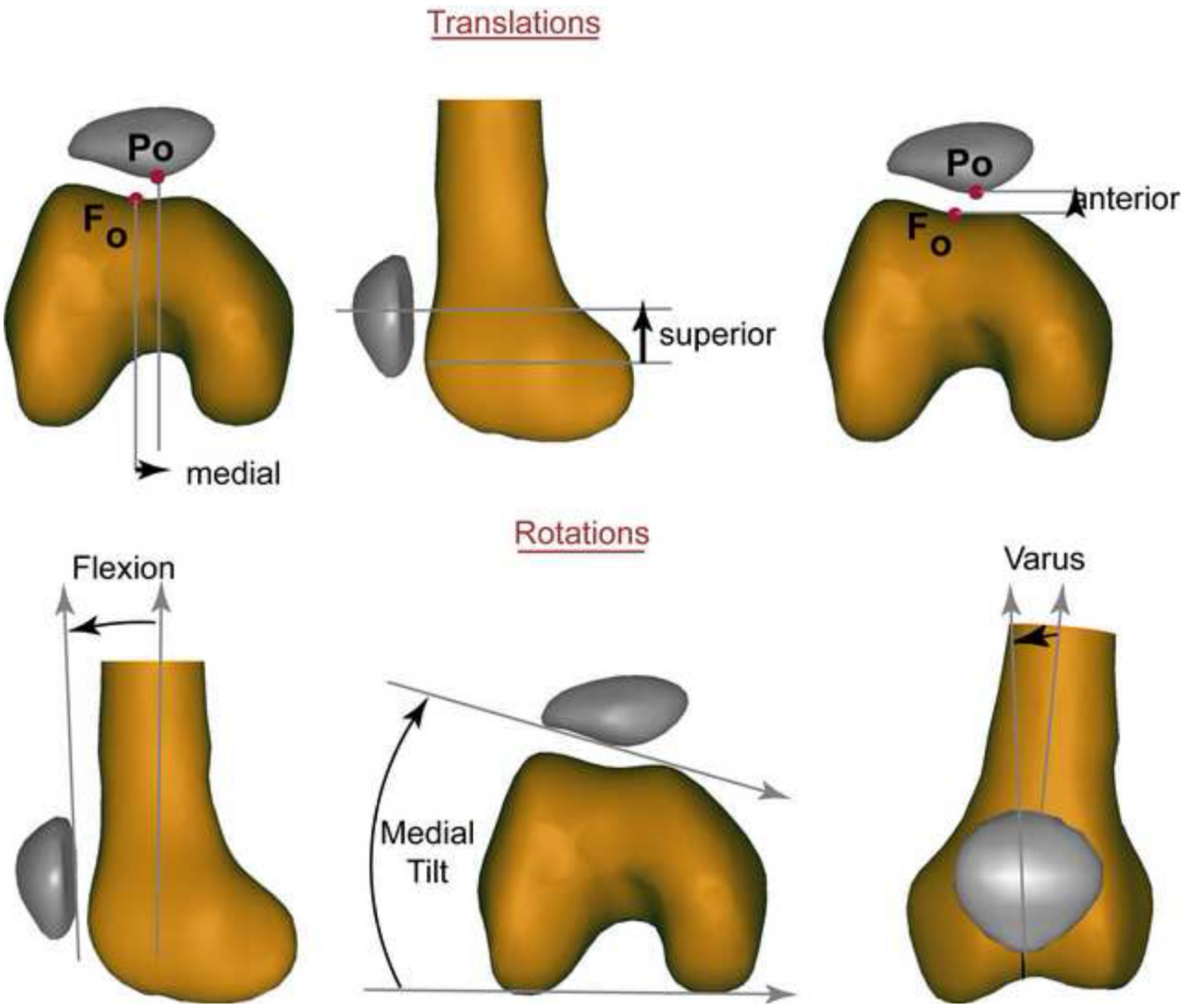

Figure 2. Two-dimensional representation of the 3D translations and rotations

The 3D orientations and translations of the patella and femur were defined relative to a coordinate system fixed in each bone (Seisler and Sheehan, 2007). This coordinate system was defined once and then the kinematics were defined through either integration of the CPC velocity data or through registration of the MPC data. The 3D patellar, femoral, and patellofemoral rotations were determined using xyz-body-fixed Cardan angles in patellofemoral kinematics (Sheehan and Mitiguy, 1999). The 3D patellofemoral rotation angles are represented in this figure by their two-dimensional counterparts.

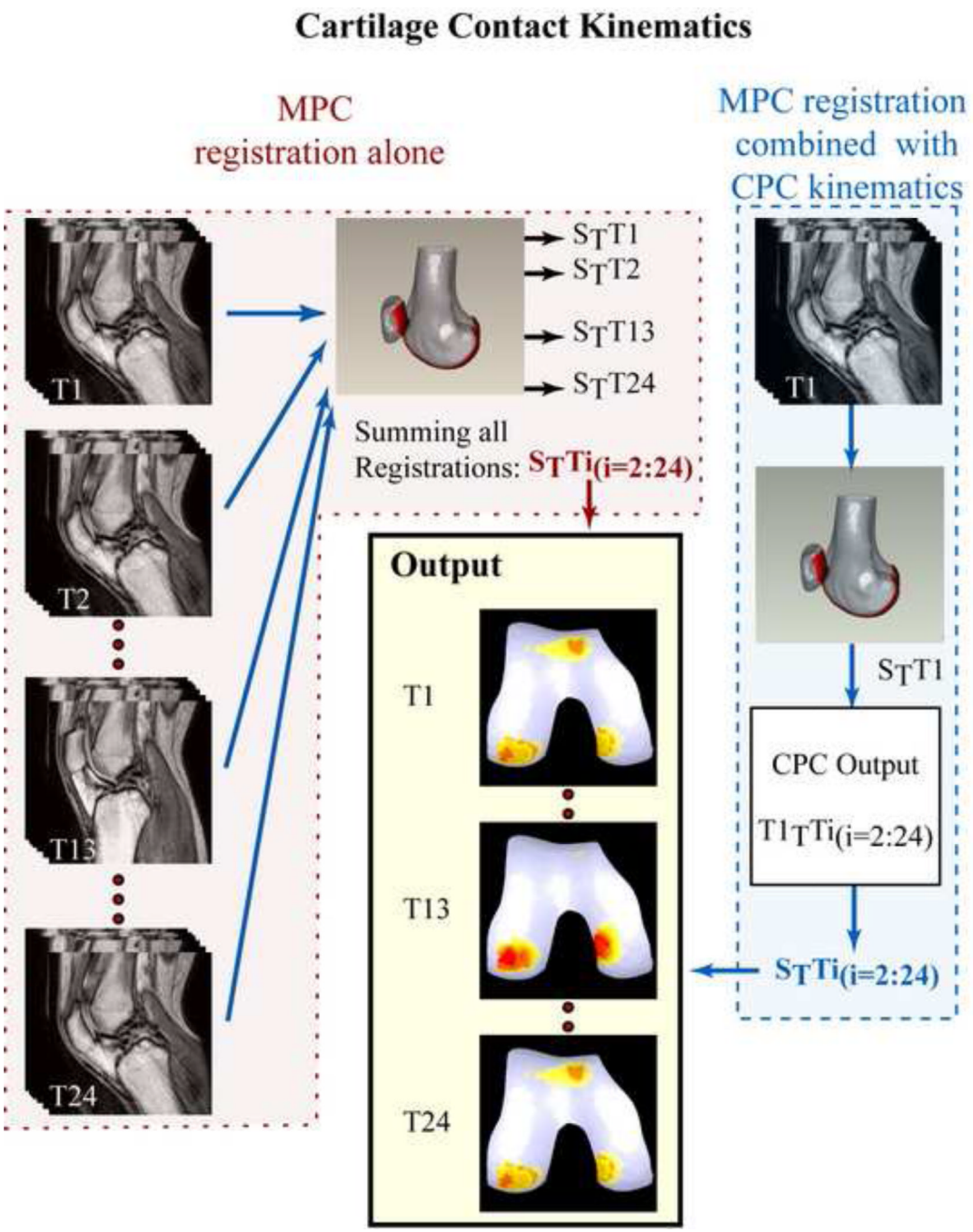

Figure 3. Quantifying Cartilage Contact Kinematics

Two methodologies (MPC registration in isolation and MPC registration combined with CPC kinematics) could apply the knee joint kinematics to the static bone and cartilage surfaces in order to calculate contact kinematics. The first methodology delineated the bone of interest in each of the MPC images and then registered each dynamic time frame to the static model (Left column registered to center 3D model):

$$^{S}T^{Ti}, i=1:24$$

$^{S}T^{Ti}$, the transformation matrix defining the transformation from a single dynamic time frame to the static model.

The kinematics of the bones were known based on the integration of the CPC data ($^{Tn}T^{Ti}$, i=2:24, n = reference time frame). Thus, the location of the bone and cartilage surfaces was known throughout the motion cycle once the registration of a single dynamic time frame to the static model was completed ($^{S}\mathbf{T}^{Tn}$, Right column), through matrix multiplication:

$$^{S}\mathbf{T}^{Ti} = {}^{S}\mathbf{T}^{Tn} * {}^{Tn}\mathbf{T}^{Ti}$$

The output of both techniques (bottom, center column) is the position of the bone and cartilage surfaces throughout the dynamic motion. Denoted on the femoral cartilage surfaces are the contact areas of the patella and tibia.

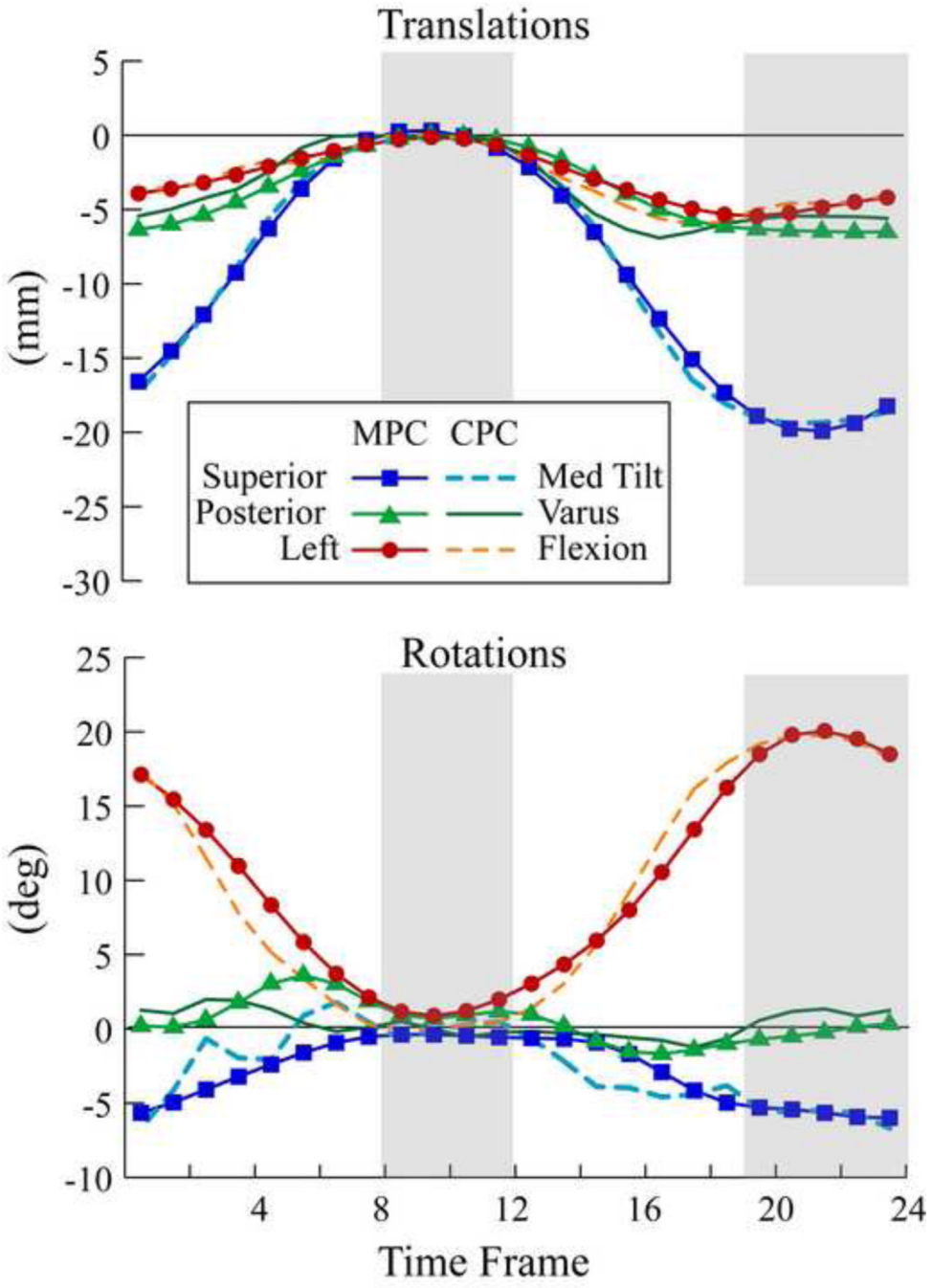

Figure 4. Patellofemoral translations and rotations for one subject using CPC- and MPC-kinematics over all (24) time-frames

The QS time frames are delineated with gray areas. Lines with no markers represent CPC-kinematics and lines with markers represent MPC-kinematics.

Table 1

Scanning parameters for dynamic magnetic resonance imaging acquisitions. The field of view (FOV), the number of slices, and the slice thickness was altered slightly between subjects based on subject size.

Scan Parameters	**CPC**	**MPC**	**MPC**
Scan plane	Sagittal-oblique	Sagittal-oblique	axial
TR	5.4	3.1	4.9
TE	2.8	1.05	1.36
Phase Direction	Anterior – Posterior	Anterior – Posterior	Anterior – Posterior
FOV	200–220 cm	200–220 cm	160 cm
NEX	2	1	1
Flip Angle (°)	12	10	20
Scan Time (min)	2.02	1.50	1.12
Recreation pixel (mm)	0.74 * 0.75	0.86*0.85	0.63 * 0.63
Views per acquisition	3	25	3
Max velocity encoding (cm/sec)	30	--	--
Number of slices	1	5 – 7	4
Slice Thickness (mm)	8 – 10	6 – 8	10
Gap (mm)	No	No	Variable

Abbreviations: CPC: cine-phase contrast; MPC: multi-plane cine TR: time to repetition, TE: time to echo, NEX: number of excitations (indicates the amount of data averaging)

Table 2

Scanning parameters for static MRI acquisition on Philips 3T scanner.

Scan Parameters	3D GRE	3D GRE
Fat Suppression	Yes	No
TR	11	11
TE	5.1	5.1
Phase Direction	Anterior – Posterior	Anterior – Posterior
FOV	140 * 140	140 * 140
NEX	1	1
Flip Angle (°)	10	15
Scan Time (min)	6.11	4.56
Recreation pixel (mm)	0.27 * 0.27	0.27 * 0.27
Number of slices	70 – 84	70 – 84
Slice Thickness (mm)	1	1
Gap (mm)	No	No

Abbreviations: GRE: gradient recall echo

Table 3

Average absolute errors ± standard deviations for patellar, femoral, and patellofemoral translations and rotations. **accuracy$_{ALL}$** represents the accuracy of the MPC registration technique in isolation and incorporated all 24 times frames. **accuracy$_{QS}$** represents the accuracy of using MPC registration from a single quasi-static(QS) time frames in combination with the CPC-kinematics to track 3D patellofemoral translation, however incorporated all the QS time-frames, where the knee angle changed less than 1.75°/time-frame.

	Translations			Rotations		
	Medial	**Posterior**	**Superior**	**Extension**	**Varus**	**Tilt**
Patellar						
accuracy$_{All}$	**0.65** ± 0.24	**0.82** ± 0.31	**1.36** ± 0.69	**1.99** ± 1.08	**1.96** ± 0.78	**2.41** ± 0.92
accuracy$_{QS}$	**0.49** ± 0.19	**0.48** ± 0.23	**0.77** ± 0.31	**1.23** ± 0.75	**1.15** ± 0.55	**1.29** ± 0.67
Femoral						
accuracy$_{All}$	**0.96** ± 0.40	**0.64** ± 0.25	**0.60** ± 0.19	**0.74** ± 0.31	**0.55** ± 0.38	**1.15** ± 0.57
accuracy$_{QS}$	**0.68** ± 0.29	**0.47** ± 0.37	**0.52** ± 0.24	**0.51** ± 0.20	**0.40** ± 0.23	**0.78** ± 0.45
Patellofemoral						
accuracy$_{All}$	**0.74** ± 0.59	**1.22** ± 0.72	**1.31** ± 0.66	**2.39** ± 1.40	**2.12** ± 0.85	**2.89** ± 1.29
accuracy$_{QS}$	**0.68** ± 0.59	**0.78** ± 0.47	**0.86** ± 0.45	**1.53** ± 0.96	**1.25** ± 0.44	**1.73** ± 1.12